

## NASA PROGRESS IN AIRCRAFT NOISE PREDICTION

J. P. Raney, S. L. Padula and W. E. Zorumski  
Langley Research Center

### SUMMARY

For several years NASA has maintained an aircraft noise prediction activity at the Langley Research Center with the goal of developing methodology for predicting the effective perceived noise level (EPNL) produced by jet-powered CTOL aircraft to an accuracy of  $\pm 1.5$  dB. Another goal is to establish, in terms of fundamental acoustic theory, the relationship of noise to the design and operation of aircraft and to demonstrate the feasibility of incorporating aircraft noise constraints into the preliminary design process. Much progress has been made toward these goals. The Aircraft Noise Prediction Program (ANOPP) contains a complete set of prediction methods for CTOL aircraft which includes propulsion system noise sources, aerodynamic or airframe noise sources, forward speed effects, a layered atmospheric model with molecular absorption, ground impedance effects including excess ground attenuation (EGA), and a received-noise contouring capability. A method for calculating noise-constrained or noise-minimized aircraft operations is presently in the validation phase. Comparisons of ANOPP calculations with measured aircraft noise levels are encouraging and highlight areas where further improvements are required.

### INTRODUCTION

In 1973, a focused aircraft systems noise prediction activity was established at the Langley Research Center. The mission was to develop a state-of-the-art computer system for calculating aircraft noise (refs. 1 and 2). The commitment to develop the Aircraft Noise Prediction Program (ANOPP) stemmed from the need for a credible means of quantifying the expected benefits from NASA's noise reduction research programs. It was also anticipated that this program could from time to time support the prediction needs of other government agencies concerned with aircraft noise and could be useful to NASA contractors.

One of the first major applications of ANOPP was to support the Supersonic Cruise Research (SCR) project at Langley; ANOPP continues to be applied to SCR research at this time. The next application was in conjunction with the FAA in an International Civil Aviation Organization (ICAO) study to determine economically reasonable and technologically feasible noise limits for future supersonic transports (ref. 3).

The ANOPP development group has a continuing commitment to assess and improve NASA's noise prediction capability. This is done by comparing predictions to measured data from both laboratory models and full-scale flight measurements. Recent prediction assessment, or validation studies, have included comparisons of prediction with flyover noise from the McDonnell-Douglas DC-9 and DC-10, the Boeing 747, and the Lockheed L-1011 aircraft.

Protocol established in conjunction with the SCR project has been improved and methodology for incorporating noise as a design constraint is being developed. An engine modeling capability which will allow investigation of the effects of variations in the relationships of engine control variables is planned, and a method for calculating noise-constrained takeoff procedures has recently been incorporated in ANOPP (ref. 4).

Several research projects which address critical weaknesses in noise prediction have been identified as a result of the focus provided by the ANOPP development and application activities. These include shock cell noise generation, ground effects on propagation, forward flight effects on jet noise, coaxial and inverted coaxial jet noise prediction, and jet-on-jet shielding effects.

The purpose of this paper is to describe ANOPP in its present state, to assess its accuracy and applicability to the preliminary aircraft design process, and to indicate where further theoretical and experimental research on noise prediction is required. The elements of the noise prediction problem which are incorporated in ANOPP will first be described. Next, the results of comparisons of ANOPP calculations with measured noise levels will be presented. Progress toward treating noise as a design constraint in aircraft system studies will then be discussed. The paper will conclude with a summary of noise-prediction-related research activities which have been initiated as a result of the need to improve aircraft noise prediction accuracy.

#### SYMBOLS

$a_j$	source noise prediction parameters
A	atmospheric propagation effects factor
$c_a$	ambient speed of sound, m/sec
D	overall source directivity factor
DI	directivity index
f	frequency, Hz
G	ground effects factor
H	altitude, m

I	source intensity, watt/m <sup>2</sup>
M	aircraft Mach number
n	number of frequency bands
P	acoustic pressure, N/m <sup>2</sup>
P <sub>ref</sub>	reference pressure, N/m <sup>2</sup>
ps	power setting, percent
R	aircraft position vector w.r.t. earth-fixed axes
r	noise propagation vector w.r.t. body axes
R	relative spectrum factor
RL	relative spectrum level (=10 log R)
S	power spectrum factor
SL	power spectrum level (=10 log S)
t	time, sec
w	weighting factor
(x,y,z)	Cartesian coordinate system
α	angle of attack, deg
β	source elevation angle, deg
θ	source directivity angle, deg
Π	acoustic power, watt
π	= 3.1415926
ρ <sub>a</sub>	ambient density, kg/m <sup>3</sup>
σ	atmospheric attenuation
φ	source azimuth angle, deg
(ξ,η,z)	cylindrical polar coordinate system
Subscripts	
f	final

i	index
max	maximum
min	minimum
o	observer
ref	reference
s	source

#### ABBREVIATIONS AND SPECIAL SYMBOLS

ANOPP	Aircraft Noise Prediction Program
CTOL	conventional takeoff and landing
$(C_L/C_D)$	lift-drag ratio
EGA	excess ground attenuation
EPNL	effective perceived noise level
ICAO	International Civil Aviation Organization
OASPL	overall sound pressure level
PNLT	tone-corrected perceived noise level
$\langle P^2 \rangle$	mean-squared pressure
SAE	Society of Automotive Engineers
SCR	Supersonic Cruise Research
SNECMA	Société Nationale D'Etude et de Construction de Moteurs D'Aviation
SPL	sound pressure level
SST	Supersonic Transport
$(T/\dot{m}c_a)$	normalized specific thrust
$(T/W)$	thrust-weight ratio

## ANOPP NOISE PREDICTION METHODOLOGY

The purpose of ANOPP is to predict noise from an aircraft by accounting for the effects of its engines, its operations, the atmosphere including ground effects, and other characteristics which may influence the noise it generates. The approach to this problem has been placed on a fundamental basis, as depicted in figure 1 (ref. 1). The aircraft follows an arbitrary flight path in the presence of an observer on the ground. During this operation, noise sources on the aircraft emit radiation with defined power, directionality, and spectral distribution characteristics, all of which may depend on time. This source noise propagates through the atmosphere (being attenuated) to the vicinity of the observer. The observer receives the noise signal from the direct ray plus a signal from a ray reflected by the local ground surface.

The essential ingredients of the aircraft noise prediction problem which are embodied in ANOPP are as follows: (1) the source intensity  $I$ , (2) the aircraft position given by vector  $R(t)$ , (3) the aircraft orientation given by  $\theta$  and  $\phi$ , (4) the atmospheric and ground-impedance characteristics given by  $A$  and  $G$ , and (5) the location of the observer given by the vector  $r(t)$ .

A number of approaches are available for this general prediction problem. These approaches are divided in ANOPP into four categories, called functional levels, which are depicted by the schematic in figure 2. The functional levels are defined by the amount of data which is processed and by the degree of approximation in the prediction methods (ref. 5). Level I predicts an effective measure of noise which depends on the observer location and assumes uniform flight conditions. Level II predicts a noise level which depends on the observer and time, but assumes standard atmospheric conditions. In Level III, frequency effects are predicted in addition to the effects of observer and time. Both nonstandard atmospheric effects and detailed flight procedures can be handled in Level III. In Levels II and III, the noise measured may be subdivided as to the noise source which generates them. Level IV predicts the same information as Level III, but with more detail in the spectral data. The present paper deals primarily with Level III noise prediction.

An ANOPP Level III noise prediction is characterized by the prediction of 1/3-octave band noise. The band centers are based on observer frequencies and are independent of time. All other inputs to the prediction modules are time dependent. The vectors from the source to the observer are naturally dependent on the observer and time so that the output from a source is a function of frequency, time, and observer.

The prediction of 1/3-octave band noise is a limitation which should not be passed over lightly. Some of the more important noise sources are actually tones, for example, from the fan rotor of a bypass-type engine. In the prediction module, these tones are assigned to a 1/3-octave band and subsequently treated as broadband noise. This will cause subsequent errors in the prediction of atmospheric attenuation, ground effects and even noise

levels. Nevertheless, the added complexity of carrying a separate procedure for tones suggests that this is not an appropriate task for ANOPP Level III and this type of analysis has been assigned to Level IV.

### Source Noise Prediction

ANOPP source modules use standard forms for the prediction equations. The standard equation of Level III prediction modules is shown in equation (1).

$$\langle p^2(f, \theta; a_i) \rangle = \rho_a c_a \frac{\Pi(a_i)}{4\pi r_s^2} D(\theta; a_i) S(f; a_i) R(f, \theta; a_i) \quad (1)$$

where

$$R(f, \theta; a_i) = \frac{S(f, \theta; a_i)}{S(f; a_i)} = \frac{D(\theta, f; a_i)}{D(\theta; a_i)}$$

The basic noise variable is mean-squared pressure,  $\langle p^2 \rangle$ . Within ANOPP, a dimensionless group is used, with  $\rho_a c_a^2$  being the reference pressure. The equation is shown in dimensional form in equation (1) so that it will be more familiar to the reader. The use of mean-squared pressure allows noise from different sources to be added directly, thus avoiding the time consuming logarithmic and exponentiation operations required to add sound pressure level, SPL.

Each noise source is characterized by an acoustic power  $\Pi$ . This power, divided by the area of a sphere with radius  $r_s$  and multiplied by the characteristic impedance of the atmosphere,  $\rho_a c_a$ , gives the average overall mean-squared pressure for virtual observers at distances  $r_s$  from the source. The power is a function of source parameters  $a_i$ , which have been previously evaluated by analysis of the engine, and the aircraft flight.

The average overall mean-squared pressure is not adequate for most predictions. It must be known how the sound is directed and how the acoustic energy is distributed in different frequency bands. This information is contained in three factors: the overall directivity factor  $D$ , the power spectrum factor  $S$ , and the relative spectrum factor  $R$ .

The overall directivity and power spectrum factors are defined in figure 3. The directivity factor is the ratio of the overall mean-squared pressure at angle  $\theta$  to the average overall mean-square pressure on the virtual observer sphere of radius  $r_s$ . The equation shown in figure 3 is for an axisymmetric source, however, ANOPP provides the directivity effects in the azimuthal direction as well as in the polar angle  $\theta$  shown here. The directivity factor is usually plotted as a directivity index, DI, which is simply ten-log of the directivity factor against  $\theta$ , the polar directivity angle.

The power spectrum factor,  $S(f)$ , is the ratio of the acoustic power in a band to the overall acoustic power. This factor may also be expressed in terms of integrals of the mean-squared pressure as shown in figure 3. Again, the equation shown is for an axisymmetric source. The integrals are used in computing  $S(f)$  from experimental data. The power spectrum factor is usually plotted in logarithmic form against frequency or Strouhal number. Since the factor must be less than one, its logarithm is negative and usually has a peak value at about -10 dB.

The overall directivity and the power spectrum give some information about how the mean-squared pressure is directed over angles and distributed over frequency bands, but this information is not complete. What is needed is either the spectrum factor for the mean-squared pressure at each angle or the directivity at each frequency band of the acoustic power. Either of these variables can be expressed in terms of the relative spectrum factor as shown in figure 4. In logarithmic form, the relative spectrum level is the difference between the mean-squared pressure spectrum level and the power spectrum level. It can be shown that this is identical to the difference between the directivity index of the frequency band and the overall directivity index. The reader may observe that many empirical prediction formulas assume a relative spectrum level of zero dB.

Forward flight effects on noise sources are not easily expressible in a standard form. This is a current research area and there is a tendency to use specialized procedures for each source. There are two definite relations, however, which distinguish the Level IV ANOPP system from the Level III and lower versions. These are shown in equations (2a) and (2b), where the subscripts o and s denote quantities at the observers and at the source, respectively.

$$f_o(M, \theta) = f_s (1 - M \cos \theta)^{-1} \quad (2a)$$

where  $a_j = a_j(M)$

is the relationship for Level IV moving source system and

$$f_s(M, \theta) = f_o(1 - M \cos \theta)^{-1} \quad (2b)$$

where  $a_j = a_j(M, \theta)$

is the relationship for Level III fixed source system. In Level IV, the frequencies are fixed at the source and the Doppler factor adjusts the observer frequency as a function of Mach number and directivity angle. In Level III, all sources are treated like broadband noise so that the observer frequency is fixed and the noise frequency is accordingly shifted by the Doppler factor. The noise source parameters in Level III may accordingly be a function of Mach number and directivity angle in some flight effect schemes.

Some of the ANOPP modules which are presently used for CTOL subsonic cruise aircraft and SST noise prediction are shown in Table I. Since the noise source modules fit within the standard form equation described previously, there is no need to go into further detail here. All ANOPP methods are fully referenceable and the reader may refer to the documents listed in Table I for full details on a particular method.

### Propagation and Noise Effects

Having discussed source noise computations, the next task is to account for propagation effects as the sound travels through a real atmosphere to an observer on the ground. It is necessary to understand how the source noise information is organized and stored, how propagation effects are included and how the resulting noise is measured and reported. The final portion of this section will compare three different noise contouring methods available in ANOPP.

Level III propagation effects. - All of the source noise prediction methods covered above calculate mean-squared pressure at a given distance  $r_s$  from the center of the source. The geometry for any of the engine sources is shown in figure 5. Since these sources are axisymmetric, it is sufficient to define acoustic pressures on a half circle centered at the center of the jet nozzle. Usually, the predicted pressures are tabulated at eighteen values of directivity angle,  $\theta$ , starting at the engine inlet axis and ending at the jet nozzle axis. Pressures are also tabulated at each 1/3-octave band center frequency from 50 Hz to 10,000 Hz as indicated in figure 6.

Level III propagation effects are represented schematically in figure 6 as correction factors which modify the near-field curve to become the far-field curve. Equation (3) contains a more detailed representation showing that mean-squared pressure at the observer equals mean-squared pressure at radius  $r_s$  multiplied by correction terms for impedance differences, spherical spreading, atmospheric attenuation, and ground effects.

$$\begin{aligned} \langle P^2(f,t) \rangle_o &= \frac{(\rho c)_o}{(\rho c)_s} \left[ \frac{r_s}{r_o(t)} \right]^2 \langle P^2(f_s(t), \theta(t); a_i(t)) \rangle_s \\ &\cdot \exp \left\{ -\bar{\sigma}(f,t) [r_o(t) - r_s] \right\} G(f_o, \beta(t), r_o(t)) \end{aligned} \quad (3)$$

where  $\bar{\sigma}$  is an average atmospheric attenuation measure and  $G$  is a ground effects factor. Notice that propagation effects must be recomputed at each time step along the trajectory because the distance from source to observer,  $r_o$ , and the elevation angle between source and observer,  $\beta$ , are changing rapidly with time. The mean-squared pressure at the source  $\langle P^2 \rangle_s$  may not

need to be recalculated at every time step since engine parameters vary slowly with time and since the variation of  $\langle P^2 \rangle_s$  with  $\theta$  can be accounted for by interpolation over a set of virtual observers.

Noise received by each observer is measured in terms of sound pressure level (SPL). Equation (4) gives a general expression for SPL and indicates two of the most common weighting functions.

$$\text{SPL} = 10 \text{ LOG}_{10} \frac{\sum_{i=1}^n w_i \langle P^2(f_i) \rangle}{p_{\text{ref}}^2} \quad (4)$$

where  $w_i = \begin{cases} 1 & \text{if OASPL} \\ w(\langle P^2 \rangle, f) & \text{if PNLT} \end{cases}$

Actually, SPL is the logarithm of a ratio of the area under a weighted mean-squared pressure spectrum and the square of the reference pressure. Level III ANOPP approximates the integral over all frequencies by a summation of integrals over each third octave band. The weights,  $w_i$ , are chosen from many possible weighting functions used to evaluate the effect of sound on humans. Overall sound pressure level, OASPL, is a flat weighting function which gives equal importance to each frequency band. Perceived noise level, PNL, is a complicated weighting function based on empirical annoyance curves. The empirical data indicate that both the frequency content and the loudness of a sound contribute to its noisiness. The measure PNLT uses the same weights as PNL but includes corrections for discrete tones in the sound spectrum.

As the aircraft flies by an observer location, the perceived noise levels will reach a peak and then subside as indicated in figure 7. Psychoacoustic research suggests that the observer reacts to the peak noise level and to the duration of the almost-peak noise levels. Effective perceived noise level (EPNL) includes this duration effect by measuring the area of the shaded region in figure 7. The prescribed method of calculating EPNL is to approximate the integral of PNLT over time by applying the trapezoid rule at half-second time intervals.

Contouring methods. - Effective perceived noise contours are useful visual aids for representing the noise level received by a large number of observers. ANOPP provides two possible avenues toward producing contour plots in a reasonable amount of computer time. The user may either use Level I approximations to calculate a large number of EPNL values or he may use the ANOPP contour enhancement methods to produce smooth contours from a limited number of accurate EPNL values. Both approaches will be discussed below.

The simplest contouring method uses Level I approximations which are based on level flyover data corrected to standard day conditions. EPNL can

be tabulated as a function of minimum approach distance,  $r_0$ , and engine power setting as pictured in figure 8. In addition to the EPNL table, the user must supply or compute aircraft position and power setting at each time step in the flight and must specify the directivity angle  $\theta$  at which the maximum noise occurs. Plotting a given contour involves interpolating into the EPNL table for the value of  $r_0$  at which that noise level occurs. The values of  $r_0$ ,  $\theta$ , and aircraft position then define an observer location as shown in figure 9. This process is repeated at each time step and the contour is drawn by a graphics subroutine which connects the observer locations.

This simple contouring method has been the accepted practice for a number of years. It is clear, however, that this method can be no more accurate than the Level I predictions on which it is based. Using this method to draw noise contours for a maneuvering aircraft or for realistic takeoff and landing operations is not recommended.

A much more powerful and versatile method is illustrated in figure 10. Noise levels are predicted for an evenly spaced grid of observer locations using either Level II or Level III prediction methods. A standard contouring computer package can draw the noise footprint from these data which are appropriate for any nonuniform aircraft operation. The major drawback of this basic contouring method is the computing cost since a dense grid of observer locations is needed to produce smooth contours. A secondary problem is the quality of the contours produced. The standard contouring software is for general purpose application and utilizes no knowledge of the basic shapes of the noise contours. These shapes are roughly concentric ellipses which are symmetric about the runway centerline. Thus the noise footprints produced rarely conform to the user's expectations.

The advanced ANOPP contouring capability overcomes the difficulties mentioned above in two ways. First, it uses a more representative coordinate system, and second, it enhances the data before contouring. The method employs the conversion from Cartesian coordinates  $(x, y, z)$  to cylindrical polar coordinates  $(\xi, \eta, z)$ . It is often advantageous to use stretched polar coordinates, achieved by dividing  $y$  by a constant before conversion to polar coordinates. By using this more natural representation, it is possible to produce reasonable contours with as few as sixteen observer locations. The ANOPP enhancement program fits a cubic surface through these sixteen points and interpolates to form a dense grid before contouring. Typical results are shown in figure 11, in which contours produced from the enhancement of sixteen calculated points compare favorably with contours produced from a very dense grid of calculated points.

## ANOPP VALIDATION AND EVALUATION

### The ICAO Study

In 1977 the International Civil Aviation Organization (ICAO) requested through its Civil Aircraft Noise (CAN) committee a recommendation for noise

standards applicable to future SST's. Participating countries included the United States, the United Kingdom, France, and the USSR. Participating organizations included Boeing Aircraft Company, McDonnell-Douglas, Lockheed, British Aerospace, General Electric, Pratt & Whitney Aircraft, Rolls-Royce, SNECMA, and NASA Langley.

A prediction subcommittee was established and given the task of choosing a "Reference Prediction Procedure" which would serve as a common denominator for the parametric studies and noise calculations supporting each participant's recommendations.

In order to provide a basis for selection of the Reference Prediction Procedure it was decided to request participants to calculate component and total noise levels for a hypothetical very low bypass ratio SST engine specified by SNECMA. Noise data for several aircraft/engine combinations were also made available to any who wished to compare predicted noise levels against measured data.

Hypothetical SST engine. - The results of the hypothetical SST engine noise calculations are summarized in Table II. Calculations were made for each of three power settings representing takeoff, cruise, and landing approach. Total flyover noise is presented in terms of effective perceived noise level (EPNL) and the component levels presented in terms of peak perceived noise level (PNL) for jet, shock cell, and combustion noise. The highest and lowest levels calculated are shown to indicate the range of the results. The levels calculated using ANOPP are also indicated.

Two conclusions were drawn from the results of the paper SST engine noise calculations. The first is that there were large differences in the noise levels predicted by different methods. The second is that ANOPP produced results which compared very favorably with the average of those calculated by other organizations.

One additional observation should be recorded. The results for fan and turbine noise were disappointing and inconclusive. The range from high to low values exceeded 20 dB with no apparent consensus as to the best method. The SST engine prediction exercise, therefore, clearly identified the need for greatly improved turbo machinery prediction methodology especially for other than jet-noise-dominated aircraft.

Comparisons with measured aircraft noise data. - Noise levels for five aircraft including Concorde and for the Aerotrain were also calculated for comparison with measured data. The procedure followed for this portion of the ICAO study was first to calculate noise levels based on input data which was provided through the chairman of the prediction subcommittee. Later, the predicted and measured perceived noise levels (PNL) were transposed to the same plot for comparison and evaluation of the accuracy of the prediction methods.

The differences between measured and ANOPP-predicted values of EPNL for all of the aircraft in the ICAO study are summarized in figure 12. On average

the ANOPP predictions were approximately 2 dB below measured levels. The dashed curve for the Concorde indicates underprediction of from 1 to 4 EPNdB depending on the jet velocity.

In summary, the ICAO study provided an early opportunity to compare ANOPP with other prediction methods and with measured aircraft data. The ICAO study also provided a basis for identifying future improvements, particularly in the turbomachinery area, in ANOPP methods. The results of the study were encouraging since the reference procedure selected by the noise prediction subcommittee in 1978 consisted mostly of ANOPP methodology.<sup>1</sup>

#### DC-9

Following the ICAO study, ANOPP noise predictions were made for a McDonnell-Douglas DC-9-32 powered by JT8D-9 so-called hardwall engines.<sup>2</sup> Noise levels, flight path, and aircraft data for actual test conditions were supplied by the manufacturer. Engine data were made available by Pratt & Whitney. Four flights of interest were drawn from a large set of tests done by McDonnell-Douglas at the Yuma test site (ref. 6). Tone corrected perceived noise level predictions were made by summing jet, core, and fan noise components. There were no shocks present. The fan noise was calculated in two stages using a modified Heidmann method, as per the ICAO recommended procedure.<sup>3</sup> Ground effects and atmospheric attenuation were included in the prediction scheme since these were present in the measured data. Finally, effective perceived noise levels were calculated.

The results of the DC-9 exercise are summarized in Table III and in figure 13. As seen in the table, the effective perceived noise levels predicted by ANOPP compare very well with the values supplied by the manufacturer. The 1 to 2 dB underprediction of EPNL value by ANOPP results primarily from an underprediction of peak perceived noise levels. The two graphs presented in figure 13 are representative. The first graph compares measured and predicted PNL as a function of radiation angle. The two curves agree very well except in the region between 100° to 130°. The second graph compares measured and predicted sound pressure level spectra for one angle in this peak noise region. The measured and predicted curves agree in general shape; however, the predicted levels average about 3 to 5 dB lower than the measured data.

---

<sup>1</sup>The final report of the Subcommittee on SST Noise Prediction was given by the chairman, M. J. T. Smith, to a meeting of ICAO noise prediction specialists at the Department of State, Washington DC, June 15, 1978.

<sup>2</sup>LTV/HTC memorandum, 1-25-79, Subject: Tone Corrected Perceived Noise Level and Sound Pressure Level Comparisons of McDonnell-Douglas DC-9 Flight Data and NASA/ANOPP Predictions.

<sup>3</sup>See Footnote 1.

## DC-10

In the first of three ANOPP validation studies for U.S. wide body aircraft, McDonnell-Douglas submitted comparisons of predicted to measured noise levels for six level flyovers of a DC-10 at power settings ranging from approach to full takeoff power (ref. 7). Inputs of noise critical engine data were prepared by the Douglas propulsion group while airplane tracking and noise data were taken from files of the flight test group. Remote computer terminal access to the Langley computer was arranged so that Douglas could run ANOPP at Langley from their Long Beach plant.

Comparisons were made on the basis of PNLT vs. angle from the inlet axis and on the basis of 1/3-octave band spectra at selected angles as shown in figure 14. Ground effects are apparent in both the predicted and measured noise spectra. EPNL comparisons were also made for each flight. Predictions included jet, fan, combustion, turbine and airframe component noise. Since the JT9D engine was installed in an acoustically treated nacelle, the effect of duct treatment was estimated. It was assumed that the duct treatment eliminated the fan tones but did not reduce the broadband noise. Even with this assumption, ANOPP tended to overpredict the high-frequency fan noise. On the other hand, the lower-frequency jet noise was consistently underpredicted. These effects are apparent in the frequency spectrum at  $\theta = 120^\circ$ . The graph of PNLT versus radiation angle in figure 14 also shows overprediction in both the forward and rear arcs which is caused by the high predicted values of fan noise. On an EPNL basis, ANOPP overpredicted from 0.4 to 3.1 EPNdB with an average overprediction of 1.3 EPNdB for the six flyovers. For the example shown in figure 14, the overprediction was 1.6 EPNdB, which is a representative case.

The DC-10 was the first aircraft for which ANOPP had overpredicted the noise. This overprediction could probably be removed by a more accurate estimate of the attenuation of fan noise provided by duct treatment. It is also possible that beneficial forward flight effects on fan noise are responsible for these differences.

## L-1011

The Lockheed-California Company participated in the second wide-body ANOPP validation study under contract to Langley Research Center. Under this contract, Lockheed selected an aircraft noise data base consisting of six flyovers at engine power settings from 60 percent to 100 percent of corrected fan speed. The noise data for these flyovers were accompanied by tracking data and engine performance information on the Rolls Royce RB-211 engines. Lockheed was linked to the Langley computer complex via a remote terminal so that the ANOPP noise prediction could be made by Lockheed's engineers.

The results of the L-1011 validation study as published in reference 8 are disappointing. While agreement between measured and predicted data at the low power settings is quite good, the noise produced at

takeoff power settings is grossly overpredicted. The difference between measured and predicted noise levels is as much as 20 PNdB for the full power takeoff case. The agreement is particularly bad in the forward quadrant, that is, for radiation angles between 20 and 80 degrees.

A study of the predicted levels of the component noise sources suggests that the overpredictions are due to high levels for the fan combination tones which are generated by supersonic tip speed fans. This explains why the low power cases, where fan tip speed is subsonic, are not overpredicted. If the Lockheed engineers had eliminated fan tones, as was done by Douglas, the results would have been greatly improved.

Figure 15 and 16 are representative of the L-1011 validation study results. Each graph contains measured data, the original predicted noise levels obtained by Lockheed and the revised predicted levels obtained by eliminating the fan combination tone or buzz-saw noise. Figure 15 contains a perceived noise level plot and a spectra plot for the full power takeoff case. Even with the revision to the fan noise prediction, the takeoff noise is overestimated in the forward quadrant. Figure 16 is included to show that for reduced power settings, ANOPP can predict L-1011 flyover noise quite well. This figure compares the measured and predicted noise spectrums at a radiation angle of 60° and a power setting of 90% fan speed. Notice that once the buzz saw noise component is suppressed, the measured and predicted curves look very similar. Even the reinforcements and cancellations caused by ground reflection are correctly predicted. This figure is typical of all the reduced power results included in the validation study.

### Boeing 747

The Boeing Aircraft Company has recently completed the third wide body validation study, which compared ANOPP predictions to 747 flyover data. The flyovers, depicted in figure 17, were made at constant 122 meter altitude (400 ft) with several engine power settings. Noise was measured by flush-mounted microphones on the airport runway. The predicted total noise was assumed to be the sum of jet, fan, core, turbine, and airframe noise components. The jet and fan noise components dominated the predicted levels in most cases.

Comparisons of predicted and measured tone-corrected perceived noise levels are shown in figure 17. At approach power, the predictions were less than the measured data at all directivity angles. The approach power prediction for EPNL was 5 dB below the measured data. At takeoff power, the perceived noise levels were overpredicted in the forward quadrant and underpredicted in the aft quadrant causing a 1 dB difference in effective perceived noise levels. No attempt to analyze the source of these discrepancies has been made except to note that buzz-saw noise was included in the ANOPP calculation by the Boeing engineers.

## Discussion

The three wide body validation studies all indicate a need for improved fan noise prediction methods. The fan noise overprediction which often reaches 10 to 15 dB is thought to result from extrapolating static test stand data to flight conditions. Acceptable results for the DC-10 were obtained because of the Douglas engineers' decision to "model" fan noise by neglecting the buzz-saw component. For the Lockheed L-1011, results were shown with and without the buzz-saw component demonstrating significant improvement when the buzz-saw component was omitted. The Boeing 747 takeoff power noise levels were apparently overpredicted in the forward arc because of the buzz-saw term.

Improvement in jet noise prediction also appears necessary. Jet noise prediction methods are based on scale model data. The wide body validation studies indicate that significant underpredictions of jet noise may result from extrapolating these model data to full-scale engines. Flight effects on jet noise appear to be another source of prediction error.

The results of the three wide body validation studies will be documented as NASA Contractor Reports and will be available for detailed analysis by the prediction community. The intent in conducting these studies was to provide a component-by-component comparison of ANOPP prediction methods with measured noise levels of current technology aircraft. The results are encouraging. Deficiencies in fan and jet noise prediction methods have been pinpointed which will provide the focus of future prediction research.

## SYSTEMS STUDIES

The application of ANOPP to preliminary design systems studies or parametric analyses is illustrated in figure 18. A few of the key dimensionless variables are the thrust-weight ratio,  $(T/W)$ , which sizes the propulsion system; the lift-drag ratio,  $(C_L/C_D)$ , which represents the aircraft's aerodynamic characteristics; and the normalized specific thrust,  $(T/\dot{m}c_a)$ , which is an indicator of source noise. The interrelationships among these and other dimensionless variables must be carefully studied before the ultimate compromise between noise at the FAA certification points, performance, and economics can be reached. The value of ANOPP for design studies and, consequently, for quantifying the benefits of proposed noise reduction technology has been established through the NASA SCR project interface and the ICAO/SCR studies. NASA is committed to continued cooperative development and improvement of ANOPP for application to future parametric and preliminary design studies of advanced aircraft system concepts.

An example of application of ANOPP to a systems study involving noise-constrained takeoff procedures is discussed in the next section.

## Optimized Takeoff Procedures

The Aircraft Noise Prediction Program has facilitated a set of systematic noise reducing trajectory studies which is unique in a number of ways. First, a standard optimization program is used to adjust continuous control functions and produce realistic takeoff solutions. Second, multiple noise constraints surrounding the runway tend to reduce noise in every direction, not just at a single point. Third, detailed mathematical descriptions of flight path, engine operations, and noise tailor the solution to a specific aircraft. Both the completeness of the studies and the approach to the problem are unique.

The general optimization problem is illustrated in figure 19. The object is to find that takeoff trajectory which minimizes noise at each selected observer location. The range of physically possible and acceptable trajectories is represented by the shaded region in figure 19. The lower limit represents a minimal adherence to accepted safety practices and the upper limit represents the maximum power takeoff. Between these extremes lies the trajectory which produces minimum noise at the observers.

A key to the solution of this general class of optimal control problems is to realize that the inverse problem is easier to solve. In other words, rather than minimizing noise at multiple observer locations with the constraint that final altitude,  $H_f$ , exceeds some minimum safe altitude, it is more natural to maximize  $H_f$  with multiple noise constraints as summarized below.

Payoff:	Maximum altitude
Controls:	$\alpha(t), ps(t)$
Constraints:	$EPNL_i < EPNL_{max} \quad i = 1, 2 \dots$
Side Constraints:	$\alpha_{min} < \alpha < \alpha_{max}$ $ps_{min} < ps < ps_{max}$

The optimization problem is to adjust the flight controls, angle of attack  $\alpha$  and power setting  $ps$ , in order to maximize final altitude while restricting the noise at each observer to some acceptable limit. The acceptable noise limit can then be lowered until no feasible solution exists. The side constraints on  $\alpha$  and  $ps$  establish a range of possible angle-of-attack values and a range of physically attainable engine settings. These constraints are equivalent to defining minimum and maximum possible trajectories bounding the shaded region in figure 19.

ANOPP is especially handy for solving optimization problems of this type. (See figure 20.) It contains a module to calculate the flight trajectory and one or more modules to evaluate Level II noise predictions at each observer. It also contains executive control statements which perform initialization

and decision logic. The optimization code, while not strictly a part of ANOPP, can be introduced to the executive system and used as any other functional module. The optimizer in use was developed at NASA Ames Research Center by Gary Vanderplaats and is described in reference 9.

The optimization approach has already been applied to advanced design supersonic transport takeoffs. The details of this research, including a description of the flight dynamics module, are contained in reference 4. One issue left unresolved in that work is the applicability of optimized procedures to present commercial aircraft. A study of the L-1011 takeoff procedures has since clarified this point.

### Optimized L-1011 Takeoff

The Lockheed L-1011 Tristar is selected for an optimized takeoff study for a number of reasons. The primary reason is that detailed engine performance and noise data are published in references 8 and 10. Moreover, the wide-body L-1011 with three high by-pass ratio RB-211 engines provides a sharp contrast to the supersonic transport concept studied previously. Finally, the L-1011 has a wide range of operating capabilities which make optimized procedures attractive. Even fully loaded, the L-1011 has a considerable amount of excess power capability so that the aircraft can maintain a climb in the event of an engine failure.

The test problem designed for the L-1011 is based on FAA certification procedures for large commercial aircraft. Two observer locations are situated along the FAR-36 sideline at 5500 m and 6000 m from brake release and a third observer location is on the runway centerline and 6486 meters from brake release. Noise levels at each observer are restricted to 96 EPNdB which proved to be the lowest feasible noise goal. (Here buzz-saw noise is omitted). Side constraints on the control functions are set very loosely at  $\alpha_{\min} = 4^\circ$ ,  $\alpha_{\max} = 16^\circ$ ,  $ps_{\min} = 70\%$ ,  $ps_{\max} = 100\%$ .

The results of the L-1011 study are presented in figures 21-23. The initial conditions are based on a representative (constant power/constant velocity) takeoff procedure found in reference 10. The ANOPP flight dynamics routine can approximate this takeoff based on the initial aircraft position and the angle-of-attack and power setting schedules given in the reference. The optimization routine then adjusts the control functions in order to maximize final altitude and to conform to the noise constraint. Initial and optimal values of angle-of-attack, power setting, altitude and velocity are given in figure 21 and 22. Notice that the optimum thrust schedule is a gradual cutback such that minimum thrust occurs slightly before the aircraft flies over the centerline microphone. The thrust schedule plus the modified angle-of-attack schedule results in a slower rate of climb than in the initial takeoff. However, the optimal solution conforms to FAA safety standards in that the climb gradient remains above 4 percent and in that the thrust cutback occurs after the aircraft has reached 213 m (700 ft) altitude.

Use of the optimal flight procedure results in reduced effective perceived noise levels everywhere along the sideline and at the flyover monitor. (See figure 23.) This test problem demonstrates the use of optimization to reduce noise levels for certification purposes. The same technique could be applied to community noise abatement studies by positioning the observer locations in areas of high population density or in areas where citizen complaints are frequent.

## NOISE PREDICTION RESEARCH

Several areas requiring further research have been identified as a result of systems studies using ANOPP to provide predicted noise levels. One of these noise-constrained or optimum takeoff procedures has been discussed in the previous section. Three others are indicated in figure 24.

### Shock Cell Noise

Shock cell noise was identified as a critical research area during the Supersonic Cruise Research studies. Shock cell noise has a nearly omnidirectional radiation pattern which causes it to dominate the forward arc during takeoff. This forward radiated noise limits the benefits of power cutback as a noise reducing operational procedure. Consequently, the elimination of shock cell noise is critical to the success of a supersonic vehicle. NASA has a strong in-house program underway which is aimed at developing the ability to understand and control shock cell noise. The initial portion of this study has been described by Seiner and Norum (ref. 11). A new theory of shock cell noise has been developed and is presently in the validation process. As indicated in figure 24 the essential feature of this new model of shock cell noise is its more forgiving nature when the exhaust nozzle is operated in off design condition.

### Lateral Attenuation Research

It became apparent during the Supersonic Cruise Research and ICAO studies that more information was needed on ground effects on aircraft noise. Quantifying the low angle of incidence phenomenon of excess (fig. 25) ground attenuation (EGA) was of particular interest. The only large data base available to check the theoretical predictions were the ground-to-ground propagation data taken by Parkin and Scholes in the mid fifties (ref. 12). There were almost no air-to-ground data available.

NASA conducted a series of flight tests at Wallops Island in 1979 in order to obtain this needed air-to-ground EGA data (ref. 13). Figure 25 shows a summary of the results of these tests in terms of a plot of the EPNdB attenuation as a function of elevation angle and distance to the

observer. Similar curves are available for the attenuation as a function of frequency. These curves agree fairly well with theory, however, there is a tendency to measure slightly more attenuation than is predicted. Also, the actual data points from the experiment show a sizable amount of scatter. The timely acquisition and interpretation of this data set has supported the development of a credible method of calculating lateral attenuation which has been documented by the SAE (A-21 Aircraft Noise Committee) in an aerospace information report (ref. 14).

Static tests were made using a source mounted on a tower at the same Wallops Island site to provide a further comparison between prediction and experiment. It is hoped that these tests will exhibit reduced data scatter and explain any remaining difference between theory and experiment.

### Jet Shielding Research

Lateral attenuation measurement on multi-engine aircraft often show greater attenuations than predicted by ground effect theory or than measured in the T-38 tests. The T-38 tests were made with only the engine nearest the microphones operating at full power so that there would be no jet shielding effect.

NASA has a program underway to determine the shielding effect of one jet on another as indicated in figure 24. An analytical study is being conducted to try to compute this effect. An in-house study is being conducted to measure the shielding of a point source. A contract study to provide experimental data of the shielding of a jet by a jet is also planned.

### CONCLUDING REMARKS

This paper has attempted to describe some of the essential features of the ANOPP system for aircraft noise prediction and to provide a basis for evaluating its present capabilities and future potential. In just a few years ANOPP has progressed from a turbojet prediction capability to its present capability of predicting the noise from high-bypass-ratio engines with coaxial flow. By virtue of participation in SCR and ICAO systems studies, procedures for incorporating noise as a constraint at the preliminary design stage have been established. A takeoff noise optimizing procedure has been developed and installed in ANOPP which calculates a minimum noise takeoff procedure subject to multiple site noise constraints.

ANOPP provides the framework in which more sophisticated source prediction theories may be evaluated when, and if, these theories show the possibility of representing experimental data over a reasonable range of test conditions. It also provides the basis for evaluating new noise reduction concepts such as inverted flow vs. conventional jets by interchanging modules so that the user immediately sees the effect on flyover noise or on a takeoff noise contour of

the inverted jet as compared to the conventional jet. The program is also useful in comparing the predictions of different theories to full-scale flight data. The ANOPP data base contains flyover spectra from three wide-body aircraft. New fan modules may be installed in ANOPP to have their predictions compared to these data. In this way, the more promising theories may be evaluated and selected for use. This procedure for the objective evaluation of noise prediction methods is an important contribution to noise research and further suggests the use of ANOPP as a means of evaluating proposed noise reduction designs and techniques.

Future activities to improve prediction accuracy include the refinement of present empirical procedures and the development of first principles prediction methodology.

## REFERENCES

1. Raney, John P.: Development of a New Computer System for Aircraft Noise Prediction. AIAA Paper 75-536, Mar. 1975.
2. Raney, John P.: Noise Prediction Technology for CTOL Aircraft. NASA TM-78700, 1978.
3. Staff of the Langley Research Center: Preliminary Noise Tradeoff Study of a Mach 2.7 Cruise Aircraft. NASA TM-78732, 1979.
4. Padula, S. L.: Prediction of Noise Constrained Optimum Takeoff Procedures. AIAA-80-1055, June 1980.
5. Zorumski, William E.: Aircraft Flyover Noise Prediction. NOISE-CON 77 Proceedings, George C. Maling, Jr., ed., Noise Control Found., c.1977, pp. 205-222.
6. Hosier, Robert N.: A Comparison of Two Independent Measurements and Analyses of Jet Aircraft Flyover Noise. NASA TN D-8379, 1977.
7. Kapper, C. Y.: Validation of Aircraft Noise Prediction Program. NASA CR-159047, 1979.
8. Godby, Larry: ANOPP Validation Study - Lockheed L-1011. NASA CR-159138, 1979.
9. Vanderplaats, Garret N.: CONMIN - A Fortran Program for Constrained Function Minimization: User's Manual. NASA TM X-62,282, 1973.
10. Shapiro, Nathan; et al.: Commercial Aircraft Noise Definition - L-1011 Tristar. Volumes I-IV. FAA-EQ-73-6, Sept. 1974. (Available from DTIC as AD A012 371 to A012 375.)
11. Seiner, J. M.; and Norum, T. D.: Aerodynamic Aspects of Shock Containing Jet Plumes. AIAA-80-0965, June 1980.
12. Parkin, P. H.; and Scholes, W. E.: The Horizontal Propagation of Sound From a Jet Engine Close to the Ground, at Radlett. J. Sound. Vib., vol. 1, no. 1, Jan. 1964, pp. 1-13.
13. Parkin, P. H.; and Scholes, W. E.: The Horizontal Propagation of Sound From a Jet Engine Close to the Ground, at Hatfield. J. Sound Vib., vol. 2, no. 4, Oct. 1965, pp. 353-374.
14. SAE Committee A-21: Prediction Method for Lateral Attenuation of Airplane Noise During Takeoff and Landing. SAE Aerospace Information Report 1751. (To be published Apr. 1981.)

TABLE I. - CURRENT LEVEL III METHODS.

<u>Module</u>	<u>Origin</u>	<u>Authors</u>	<u>Documentation</u>
Single Jet	Boeing/SAE	Jaeck/Tanna	SAE ARP 876, Boeing Doc. D6-42929 J. Sound Vib 50.3, 1977.
Coaxial Jet	NASA	Stone	NASA TM X-71618
Inverted Jet	NASA/Kentron	Pao/Russe11	NASA TP 1301, NASA CR 3176
Fan	NASA	Heidmann	NASA TM X-71763
Combustion	GE/FAA/SAE	Matta/Cornell	SAE ARP 876 FAA RD-77-4, FAA-RD-74-125-III
Turbine	GE/FAA/Kentron	Matta/Rawls	FAA-RD-77-4, FAA-RD-74-125-III
Airframe	UTRC/FAA	Fink	FAA-RD-77-29
Attenuation	Wyle/DOT/ANSI	Sutherland	DOT-TST-75-87, ANSI STD S1.26
Ground Effects	NASA	Pao/Willshire	NASA TP-1104, NASA TP 1747

TABLE II. - RESULTS OF THE HYPOTHETICAL SST ENGINE ICAO NOISE PREDICTION EXERCISE.

	Freefield Total Noise EPNL	Jet	Freefield Source Noise	
			Shock	Combustion
100% Power	High	116	114	101.5
at	Low	110	110	95
305 m (1000 ft)	ANOPP	113	112.5	96
66% Power	High	106	96	97
at	Low	98.5	84	91
305 m (1000 ft)	ANOPP	101	96	91.5
25% Power	High	100	NA	99
at	Low	84	NA	92
122 m (400 ft)	ANOPP	93	NA	92

TABLE III. - COMPARISON OF PREDICTED AND MEASURED EPNL VALUES.

Run No.	ANOPP	Measured (McDonnell-Douglas)
Takeoff		
1	96.7	97.9
2	95.7	97.1
Landing		
3	102.8	102.3
4	100.1	102.4

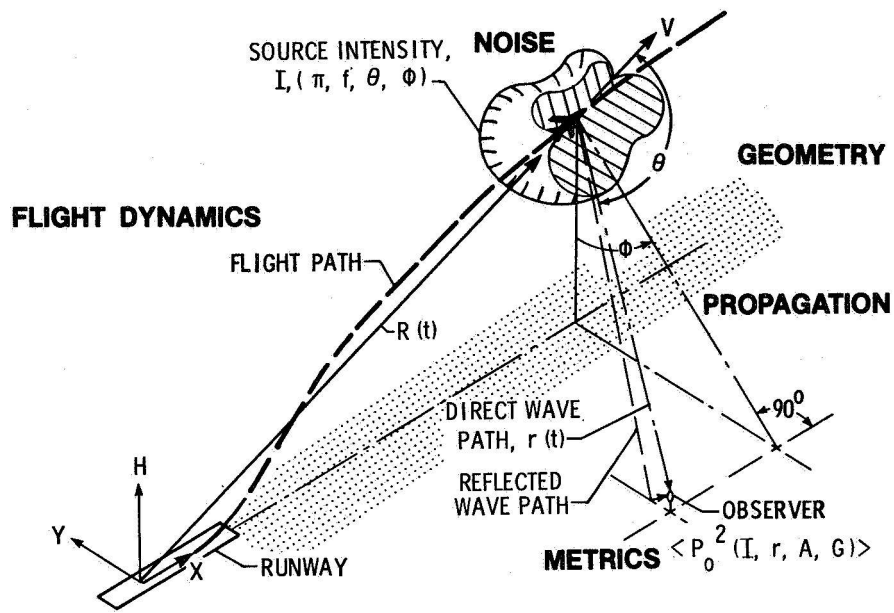


Figure 1.- ANOPP prediction methodology.

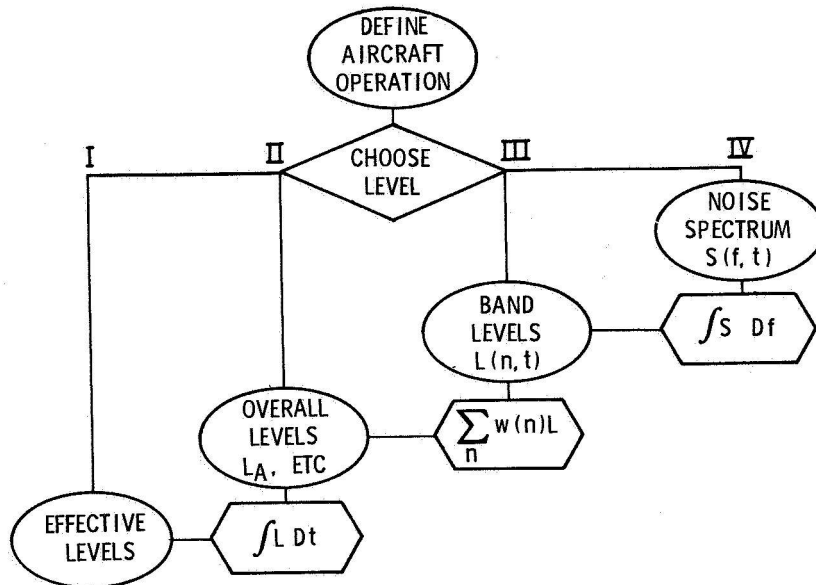


Figure 2.- ANOPP functional level computation flow diagram.

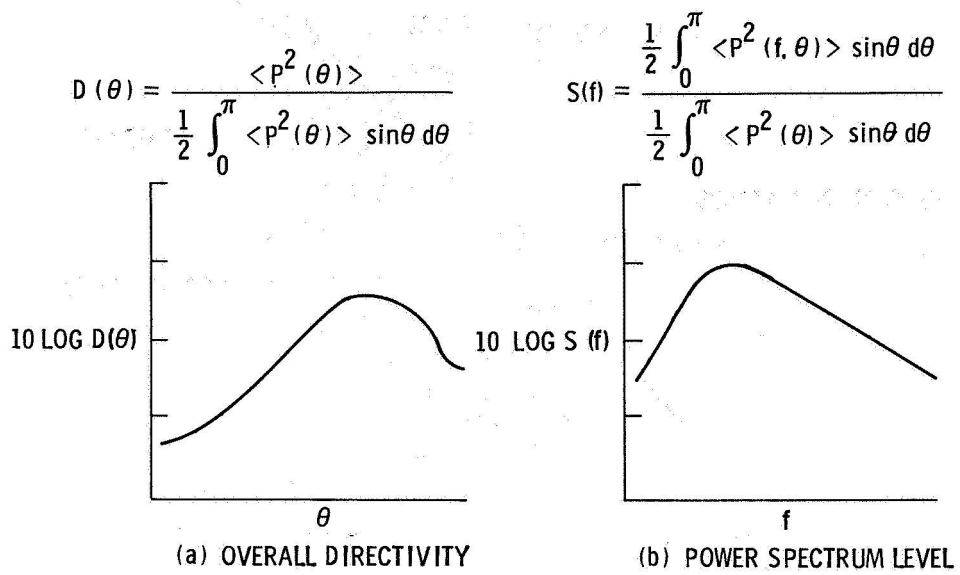


Figure 3.- Overall directivity and power spectrum levels.

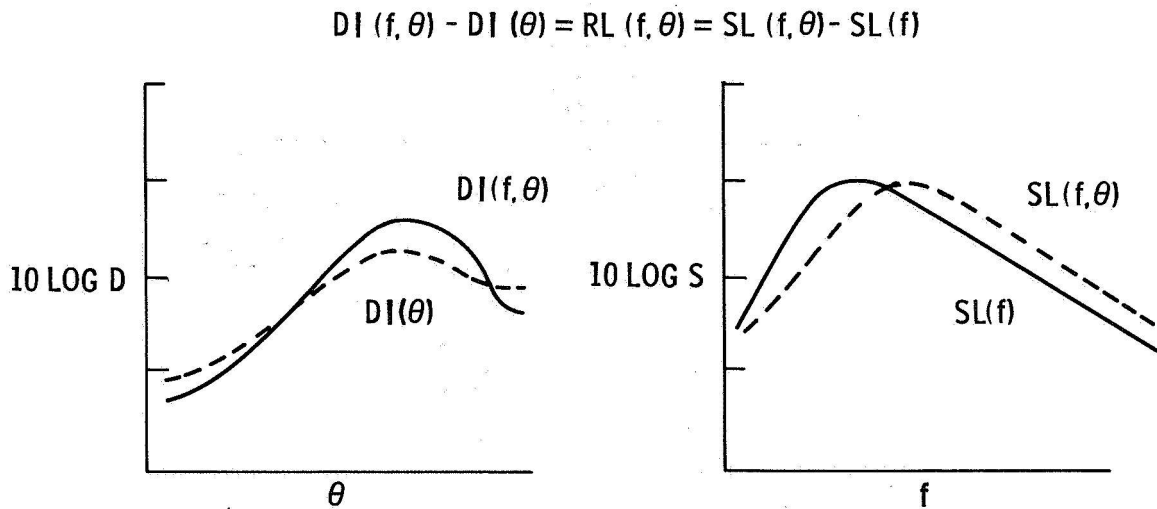


Figure 4.- Relative spectrum levels.

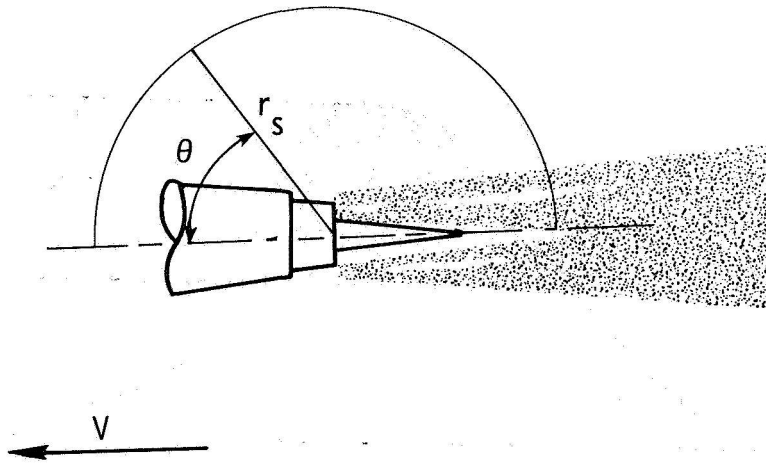


Figure 5.- Source noise prediction geometry.

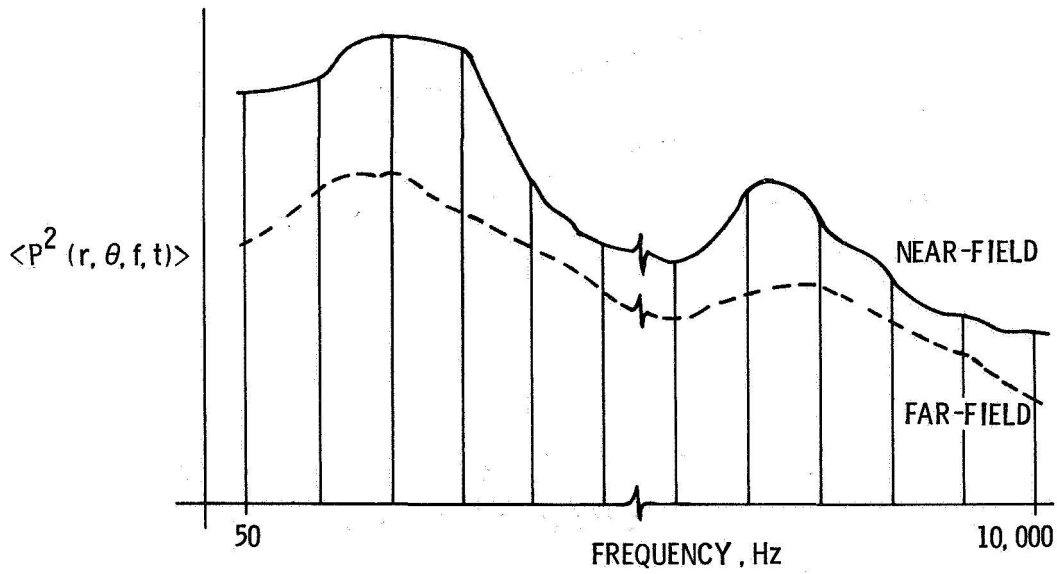


Figure 6.- Near-field and far-field noise spectra.

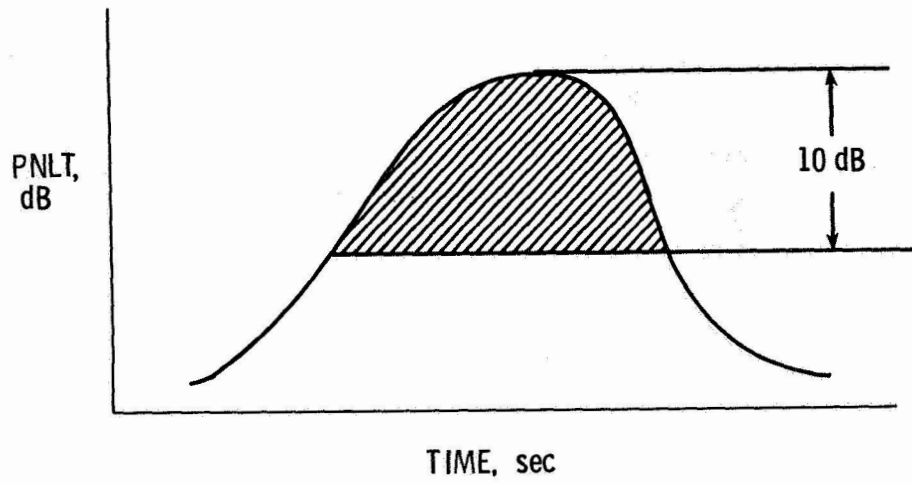


Figure 7.- Effective perceived noise level computation.

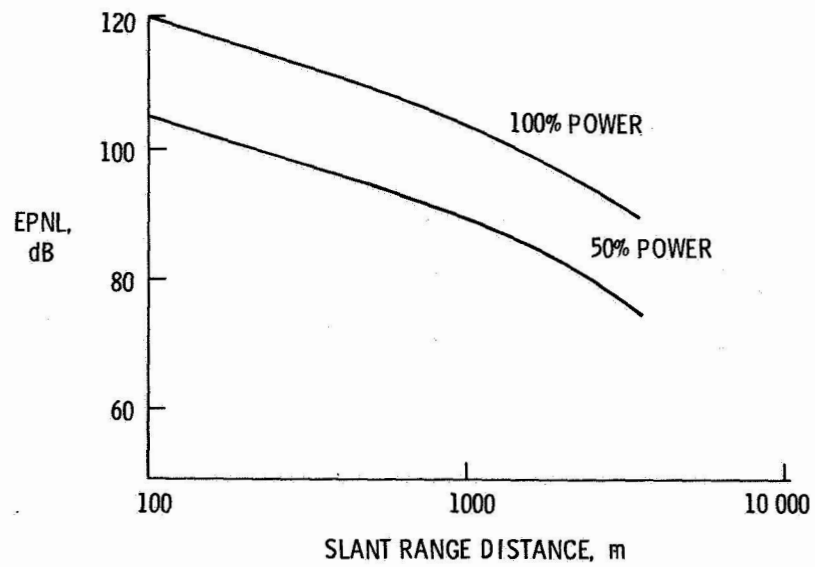


Figure 8.- Noise level/slant range curves.

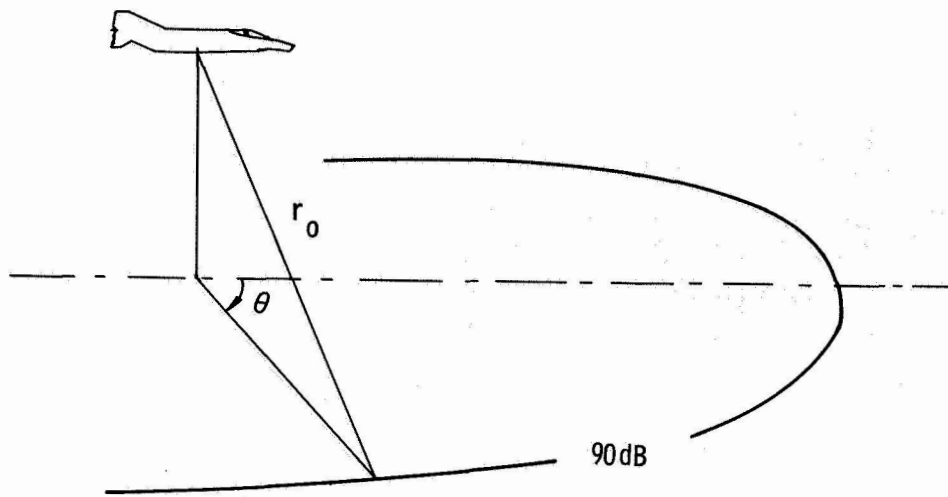


Figure 9.- Level I contouring procedure.

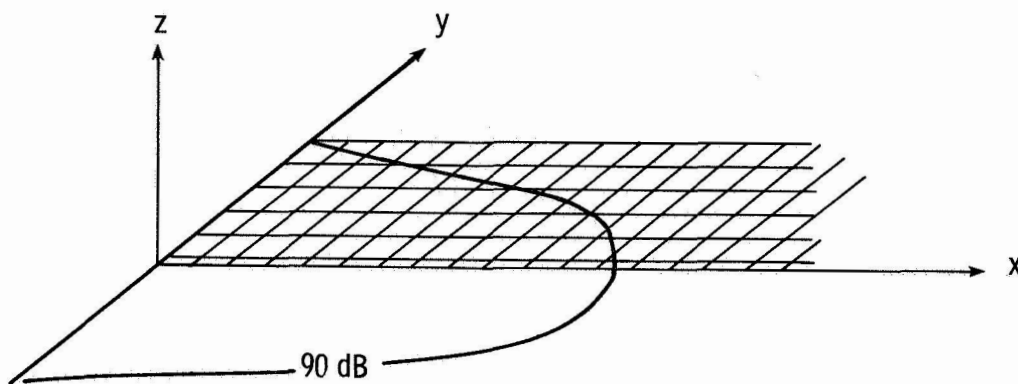


Figure 10.- Level II and III grid contouring method.

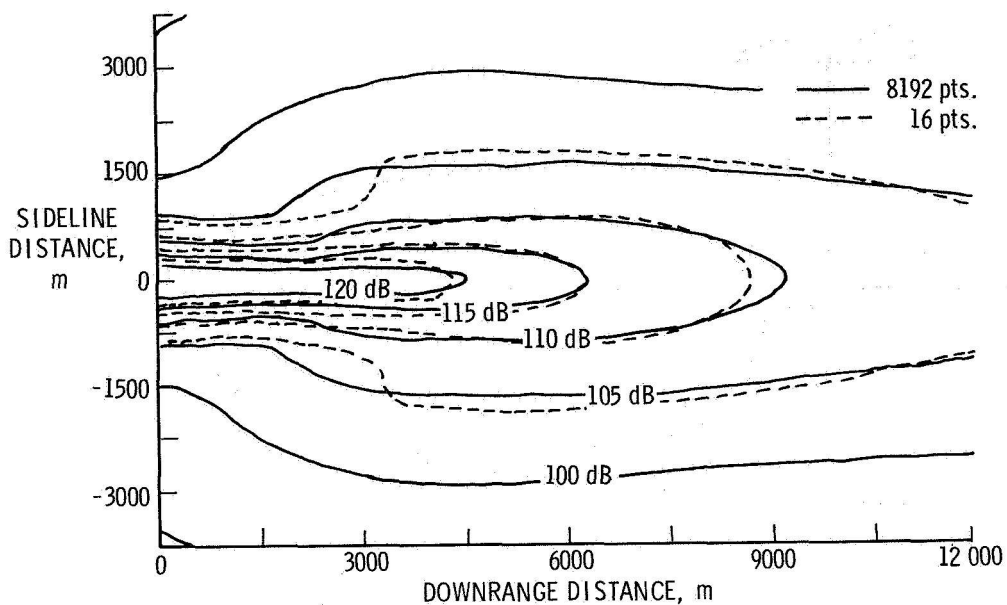


Figure 11.- Comparison of ANOPP enhanced EPNL contours with very accurate nonenhanced contours.

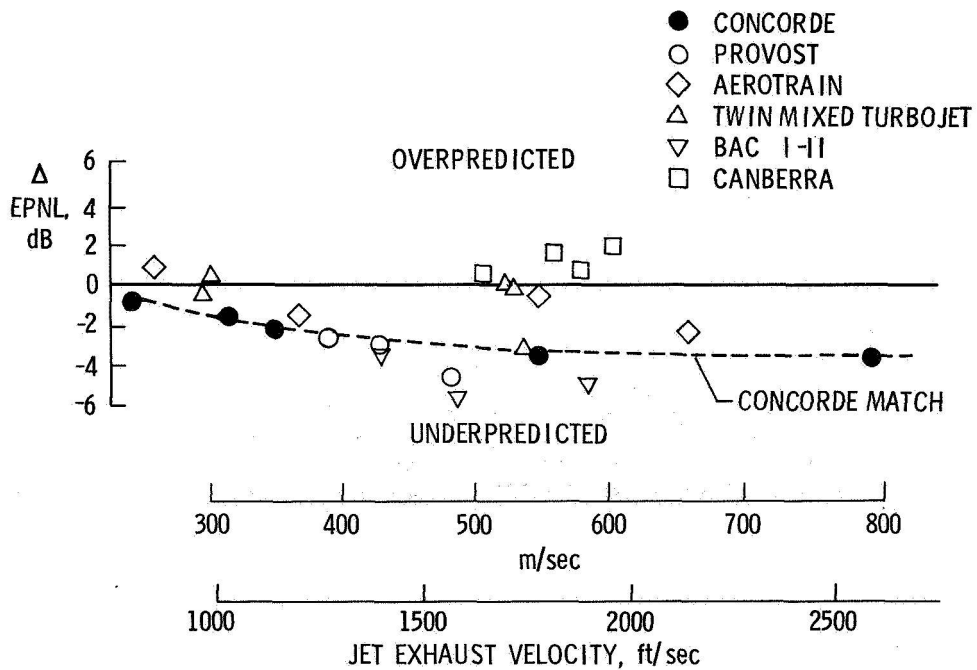


Figure 12.- Comparison of ANOPP predictions with measured data in the 1977 ICAO exercise.

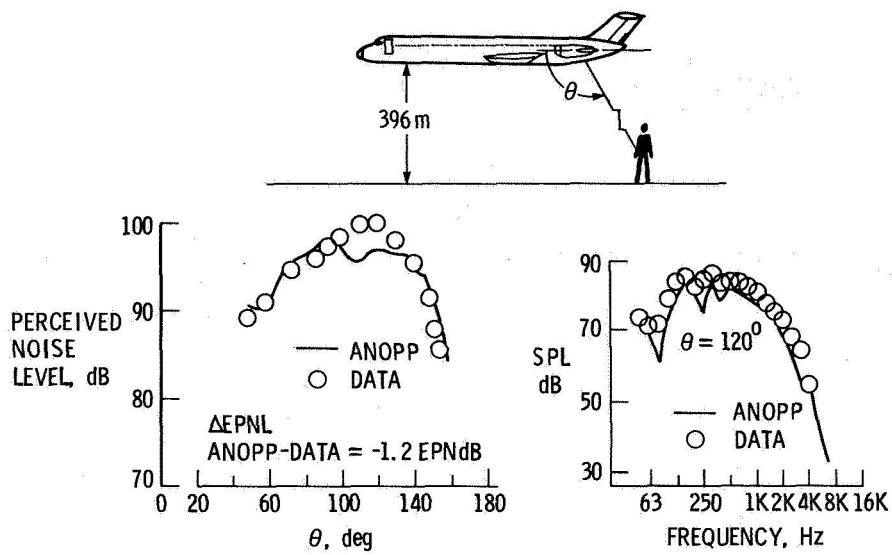


Figure 13.- Comparison of DC-9 noise prediction with measured data.

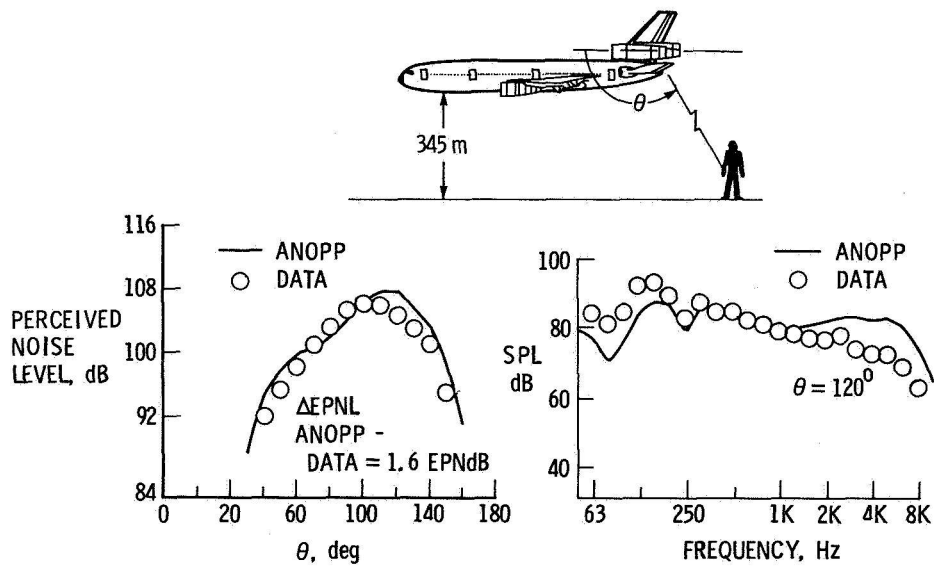


Figure 14.- Comparison of DC-10 noise prediction with measured data.

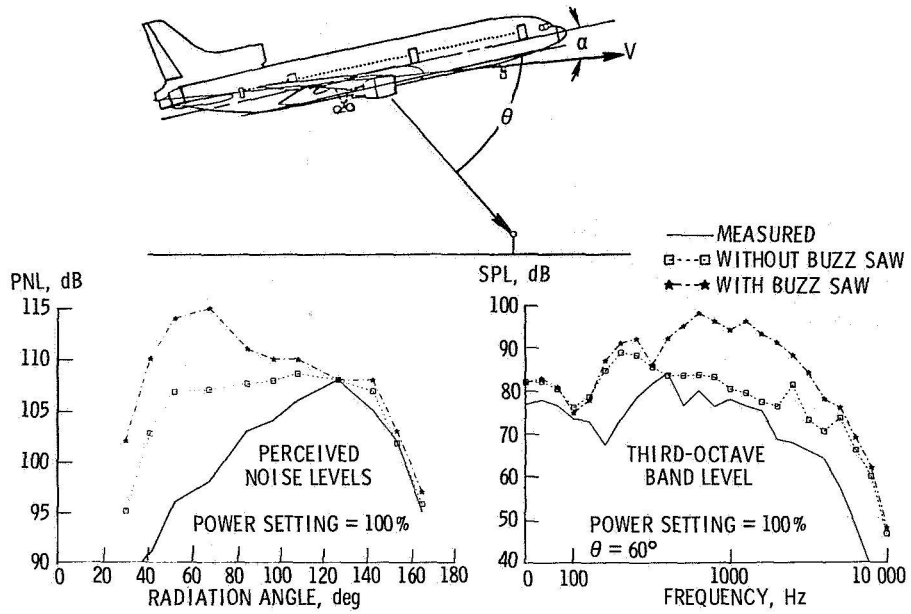


Figure 15.- Comparison of L-1011 noise prediction with measured data.

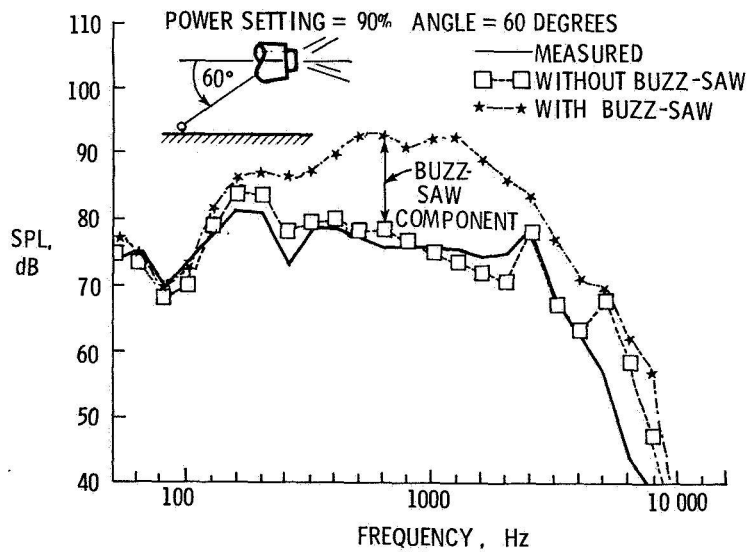


Figure 16.- L-1011 noise spectra for a reduced power flyover.

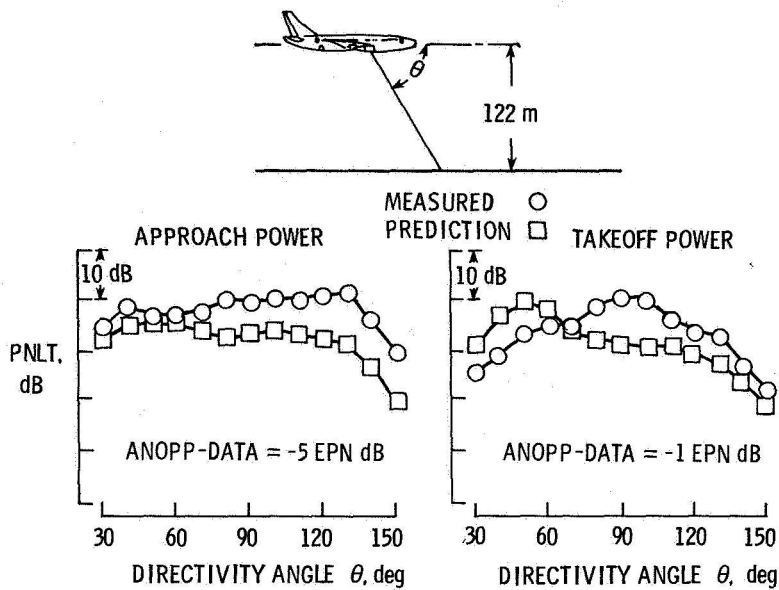


Figure 17.- Comparison of 747 noise prediction with measured data.

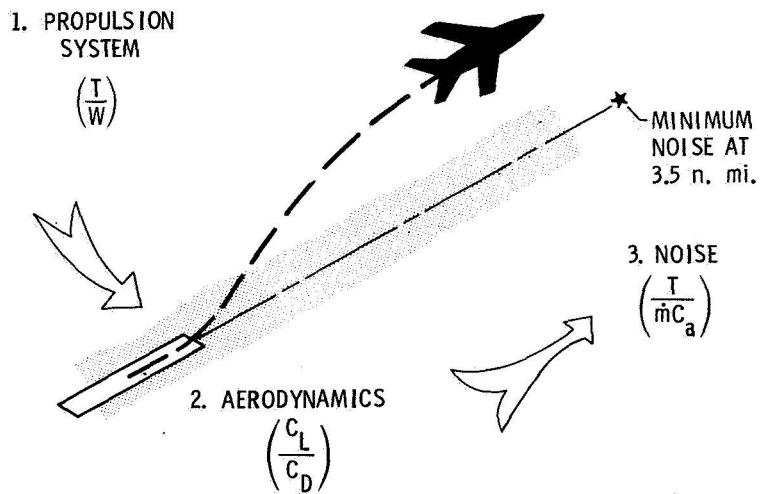


Figure 18.- ANOPP preliminary design systems studies.

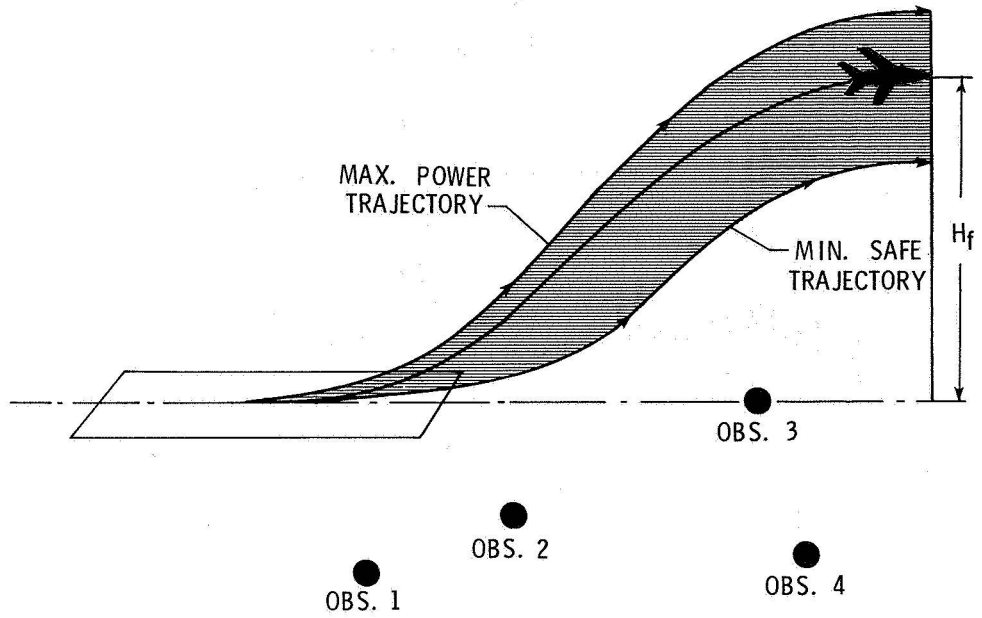


Figure 19.- Noise reducing operational procedures.

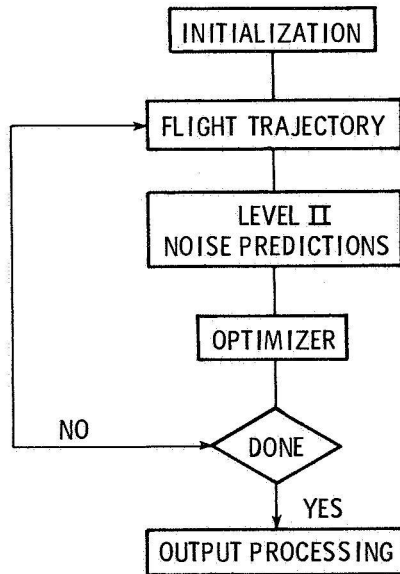


Figure 20.- Flow of the optimization computations.

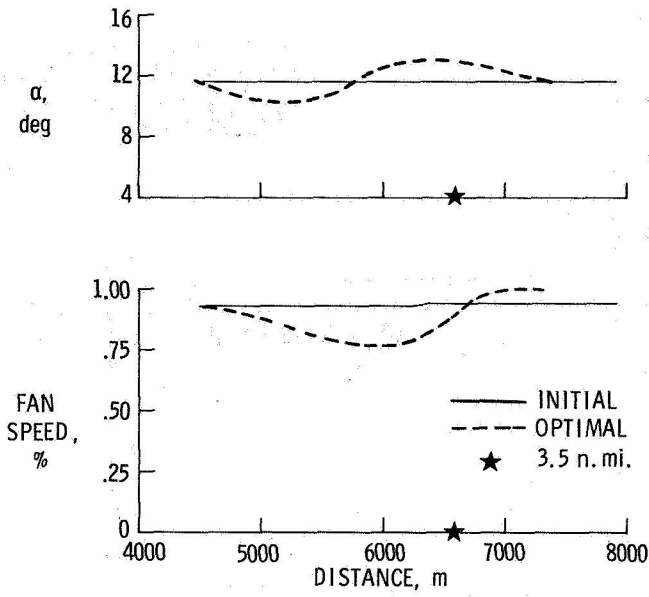


Figure 21.- Comparison of initial and optimal control functions.

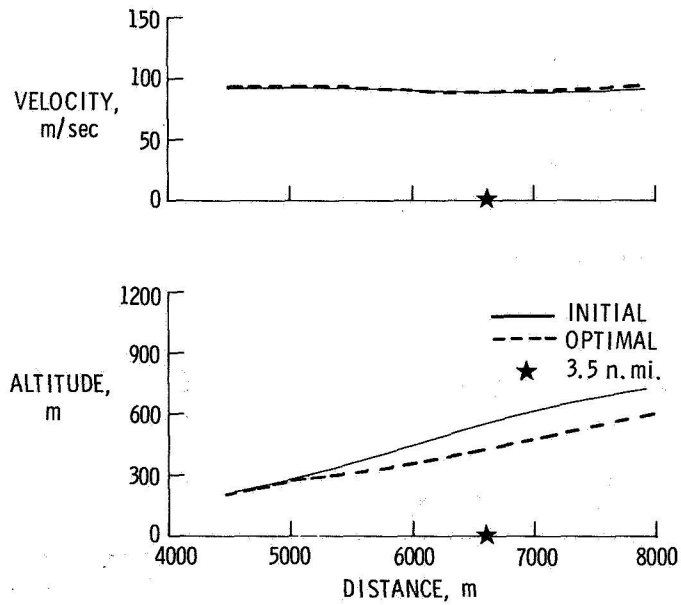


Figure 22.- Effect of optimal controls on L-1011 flight performance.

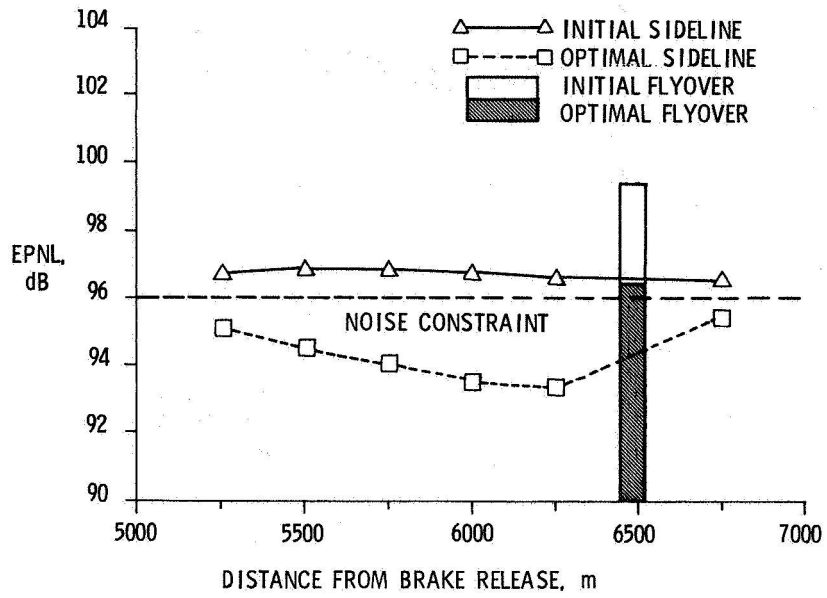


Figure 23.- Noise reduction obtained from optimized flight procedures.

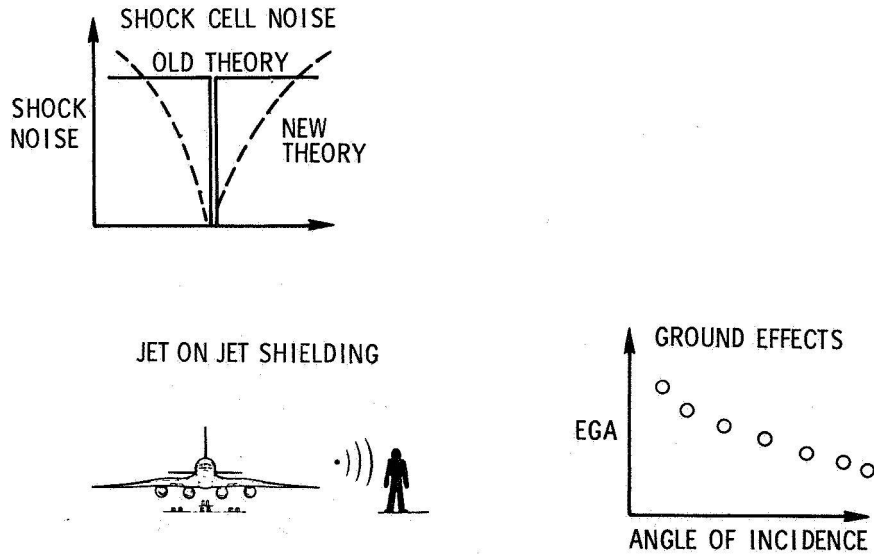


Figure 24.- New research areas identified by ANOPP.

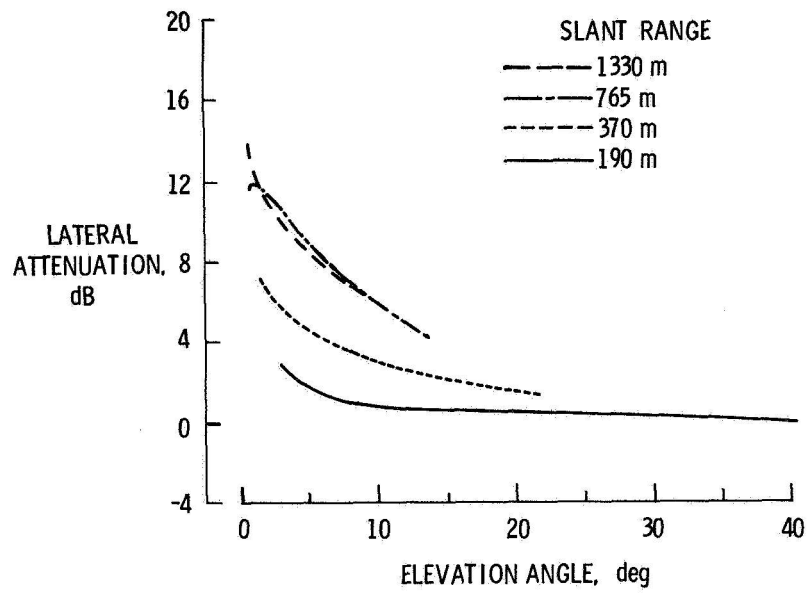


Figure 25.- Lateral attenuation in T-38 flyover data.

